*Journal of Low Temperature Physics, Vol. 86, Nos. 3/4, 1992*

# Circular Dichroism and Birefringence in Unconventional Superconductors

**S. K. Yip and J. A. Sauls**

*Science and Technology Center for Superconductivity and Department of Physics & Astronomy, Northwestern University, Evanston, Illinois*

(Received October 3, 1991)

*We present a theoretical analysis of circular dichroism and birefringe in unconventional BCS superconductors with appropriate broken symmetries. We show that for the effect to exist, that in addition to broken time-reversal and two-dimensional parity symmetries, it is necessary to take into account the weak particle–hole asymmetry of the low-energy excitations of the metallic state. Circular dichroism and birefringence are shown to arise from the order parameter collective mode response of the superconductor; in the clean limit the contribution to the current response from the single-particle excitations does not give rise to circular dichroism or birefringence, even with particle–hole asymmetry. The magnitude of the circular dichroism is found to be small for the classes of superconductors which are thought to be likely candidates to exhibit the requisite broken symmetries, namely the heavy fermions and oxide superconductors. The order of magnitude of the elliptical polarization of a linearly polarized incident wave is* $v_f/c(\xi/\lambda_L)(\Delta/E_f)\ln(E_f/\Delta)$, *which is roughly* $10^{-7}$–$10^{-8}$ *rad at frequencies of order the gap, and decreases at least as fast as* $(2\Delta/\omega)^2$ *at higher frequencies.*

## 1. INTRODUCTION

The physical properties of nearly all known superconductors are successfully explained by the BCS theory, the central feature of which is the formation of a condensate of Cooper pairs which spontaneously breaks gauge symmetry.[1,2] However, in the original theory, except for the broken gauge symmetry, the superconducting state has the full symmetry of the corresponding normal metallic phase. Since BCS proposed their theory, there have been numerous theoretical proposals and experimental searches for "unconventional" superconductors in which the condensate spontaneously breaks additional symmetries of the normal phase. In recent years this



0022-2291/92/0200-0257$06.50/0 

possibility has been actively pursued for the heavy fermion superconductors, where there is now considerable, but not conclusive, evidence for a multi-component order parameter associated with an unconventional superconducting ground state.[3–5] There have also been theoretical papers arguing that the high $T_c$ oxide superconductors are unconventional BCS superconductors;[6] however, the evidence is less conclusive than that of the heavy fermion superconductors.

Numerous tests have been proposed to identify unconventional superconductivity, but so far the only unambiguous unconventional superconductor is superfluid $^3$He, which is well established to be a spin-triplet, p-wave pair condensate exhibiting broken spin and orbital rotation symmetries, and broken time-reversal symmetry in additional to broken gauge symmetry.[7] The most definitive tests of unconventional pairing are measurements of a physical property of the superconducting state which exhibits a lower symmetry than the underlying normal metal. In particular, Gorkov[8] proposed that measurements of anisotropy in the upper critical field of a superconductor with a cubic or tetragonal point group would indicate an unconventional order parameter with lower rotational symmetry than that of the crystal. Similar proposals for measuring anisotropies in the London screening length[9] or thermoelectric effects[10,11] as measures of broken rotational symmetry have been made. Recent theories[12–15] of the superconducting phases of $UPt_3$ are based on a two-component order parameter that spontaneously breaks time-reversal symmetry, as well as elements of the point group, and several proposals to detect broken time-reversal symmetry were put forth. Choi and Muzikar showed that non-magnetic impurities, in an unconventional superconductor with broken time reversal symmetry, would deform the pair condensate and generate supercurrents, resulting in a local field at the impurity, which in principle could be detected as an NMR or $\mu$SR frequency shift.[16] Similarly, Tokuyasu *et al.*[17] showed that the same internal orbital currents that are connected with the induced magnetic field at an impurity would also interfere with the supercurrents that generate the flux of a vortex line, the result being that the lower critical field, $H_{c1}$, for flux to enter a superconductor depends on the relative orientation of the external field and the spontaneously broken symmetry axis about which the pairs orbit; this asymmetry in $H_{c1}$ would be strong evidence for broken time reversal symmetry of the superconducting state. To date, however, there are no experiments that have yielded a positive, unambiguous identification of the order parameter of an unconventional superconductor (other than superfluid $^3$He).

A theory of superconductivity, not based on the phenomenon of pair condensation, has been proposed largely in response to the discovery of high-temperature superconducting oxides[18] (see Ref. 19 for a detailed list of

references). In this theory superconductivity is a consequence of exotic statistics (half-fractional statistics) that is presumed to describe the elementary excitations (anyons) of the two-dimensional (2D) CuO sheets from which most of the oxide superconductors are built. A central feature of the anyon model is spontaneously broken time-reversal (T) and parity (P) symmetries that are direct consequences of the statistics. Wen and Zee[20] pointed out that these systems may then have circular dichroism and birefrigence; i.e., that right and left circularly polarized EM waves, when incident on the material in question, are reflected with different intensities and/or phase angles. Halperin *et al.*[19] have examined in more detail the possible consequences of broken T- and P-symmetries for anyon superconductors. This association between anyon superconductivity and broken T- and P-symmetries has stimulated several experimental searches for these signatures. Experiments searching for circular dichroism and birefringence have been reported by three groups.[21–24] However, the experimental details and the results differ, and there is no obvious simple model capable of explaining all the experiments. Thus, so far no definitive conclusions have been reached about the existence or non-existence of a superconducting state exhibiting broken time-reversal and/or broken parity symmetry, much less any definitive conclusion about the relevance of the anyon model to high $T_c$ superconductivity.

It should be emphasized that the anyon model is not the only possible superconducting ground state that exhibits broken T- and P-symmetries that may be realized in the oxide superconductors, or any other candidates for exotic superconductivity. Many models of unconventional BCS superconductivity that have been investigated (in the context of heavy fermion superconductivity and to some extent the oxides) are pair condensates with broken T- and P-symmetries. In fact, if superfluid $^3$He–A were a charged fluid, it would exhibit, among other novel phenomena, circular dichroism and birefingence. So it is important for the current debate about the nature of superconductivity in the high $T_c$ oxides to recognize that positive confirmation of broken symmetry in the superconducting state does not tell one much more about the nature of the ground state, at least not without a more quantitative theory of the signatures of the associated broken symmetries.

This leads us to the main purpose of this report. We have calculated the circular dichroism and birefringence that one expects to observe from a good type II superconductor with an unconventional BCS order parameter possessing broken T- and P-symmetries. We confine our analysis to cases where the electromagnetic radiation is propagated along a high symmetry direction, i.e. an axis with at least three-fold rotational symmetry, and where this rotational symmetry is either unbroken in the superconducting state, or can be restored by a gauge transformation. These assumptions, although

restrictive, are consistent with many of the proposals for the superconducting states of the heavy fermion superconductors as well as the high $T_c$ superconductors. If the superconductor does not respect this additional rotation symmetry, then the system will exhibit *linear* dichroism and birefringence. The observation of circular dichroism or birefringence requires broken 2D parity and time-reversal symmetries. We also show that this effect vanishes identically if the normal metallic state is assumed to be invariant under the interchange of particles and holes (i.e. is particle–hole symmetric). Thus, it is necessary to consider particle–hole asymmetry effects. We find that the excitation contribution of the current response (the "empty bubble" in Green's function language) has particle–hole asymmetric terms that are identical for both circular polarizations. We call these "trivial" particle–hole asymmetric terms, in contrast to the "non-trivial" particle–hole asymmetric terms which differ for the two circular polarizations. These later contributions are due entirely to the collective-mode response of the order parameter (these are the vertex corrections in Green's function language).

We demonstrate these general features with an explicit calculation for a representative order parameter with broken time-reversal and 2D-parity symmetries, namely the Anderson–Brinkman–Morel (ABM) order parameter[25] (which also describes the A-phase of superfluid $^3$He). The broken symmetries are exhibited by a condensate of pairs all having orbital angular momentum $l_z = \hbar$ about a fixed spatial direction. Although the ABM state is a spin–triplet pair-condensate, the spin structure of the order parameter is irrelevant for the electromagnetic properties we are interested in. In fact the ABM order parameter is representative of a large class of unconventional superconducting states (even- or odd-parity) exhibiting broken T- and P-symmetries. Thus, the qualitative features and order of magnitude of the circular dichroism are not specific to any particular state, and our preliminary investigation of other states bears this out. The theoretical result for the magnitude of the circular dichroism is small. For a linearly $\hat{x}$-polarized incident wave, the relative magnitude of the $\hat{y}$-polarized reflected wave amplitude is of order $(\Delta^2/\omega_P E_F)(\xi/\lambda_0)^2 \ln(E_F/\Delta)$ for $\omega \sim \Delta$ where $\Delta$, $\omega_P$, $E_F$, $\lambda_0$, $\xi$ are the energy gap, plasma frequency, Fermi-energy, London penetration depth and coherence length respectively. This is a small amplitude, of order $10^{-7}$–$10^{-8}$ for parameters appropriate to the oxide superconductors, compared with $10^{-(4-5)}$ in experimental reports[21,22,24] of circular dichroism and birefringence. For $\omega > 2\Delta$, the magnitude of the circular dichroism decreases at least as fast as $(2\Delta/\omega)^2$. If the reports of this effect in the high $T_c$ oxides are indeed due to the superconducting state, then it almost certainly requires a different theory of the superconducting state than that of an unconventional BCS order parameter. Any theory capable of generating optical dichroism and birefringence from superconductivity with magnitudes the

size reported in Refs. 21, 22, and 24 must involve internal currents (responsible for broken T- and P-symmetries) which are much stronger than one would estimate on dimensional grounds from an energy scale, $k_B T_c$, and length scales, $\xi$ and $\lambda_L$.

Because the circular dichroism and birefringence reported here relies on particle–hole asymmetry and involves parameters that are generically small for both the oxide superconductors and the heavy fermions, the magnitude of the circular dichroism is probably beyond present experimental capabilities. It is hoped, however, that these capabilities can be improved in order to search for this effect, particularly in the heavy fermion superconductors. For if circular dichroism were observed to appear in the superconducting phase that would be convincing evidence for unconventional superconductivity exhibiting broken time-reversal and 2D parity symmetries.

The paper is organized as follows. In Sec. 2 we discuss the relevant symmetry relations applicable to the electromagnetic response function, and identify the symmetries that need to be broken in order for a superconductor to exhibit circular dichroism and birefringence. In Sec. 3 we present the microscopic theory for the current response of a clean superconductor with an order parameter that spontaneously breaks the necessary symmetries required for circular dichroism. We relate this response function to the reflectivity of electromagnetic radiation that is incident normal to the surface in Sec. 4, and discuss the results of numerical calculations in Sec. 5.

## 2. SYMMETRY ANALYSIS

Consider a plane EM wave directed along the surface normal (which we also assume to be a high symmetry direction) of a good type II superconductor, i.e. $\lambda_L \gg \xi$. The EM field typically penetrates deep into the superconductor and probes the bulk order parameter. Effects associated with the surface region (thickness $\sim\xi$) where the order parameter may be strongly deformed are ignored here. In this case we can analyze the symmetry conditions obeyed by the current response of the superconductor with a spatially uniform order parameter. The role of the surface is then described by a boundary condition on the EM field which we discuss in Sec. 4.

To calculate the reflectivity of electromagnetic radiation one needs the current–current response function of the system, which consists of paramagnetic and a diamagnetic part. Since the diamagnetic part has the same symmetry as the crystal itself and has identical values in the normal or any superconducting state, we need only discuss the paramagnetic response

function defined by the Kubo formula,

$$K_{ij}(\mathbf{q}, \omega; \Delta) = -i \int_{-\infty}^{\infty} dt \int_{-\infty}^{\infty} dz\, e^{i\omega t - iqz} \Theta(t) \langle [J_i(z, t), J_j(0, 0)] \rangle \qquad (1)$$

where $i, j$ denote the spatial components of the current and $\Theta(t)$ is the step function. The arguments of $K_{ij}$ indicate that the response is evaluated for the wavevector $\mathbf{q} = q\hat{z}$, frequency $\omega$, and in the superconducting state with an order parameter specified by $\Delta$ (which is in general a complex spin matrix). We confine ourselves to wavevectors along the symmetry direction specified by $\hat{z}$, which is assumed to be an axis with at least three-fold rotational symmetry. Thus, the normal state response is proportional to the unit matrix (i.e. $K_{xx} = K_{yy}$ and $K_{xy} = K_{yx} = 0$).

We confine ourselves to the superconducting states in which this rotational symmetry is preserved up to a gauge transformation; otherwise, the response would be anisotropic in the $x$–$y$ plane, in which case the system exhibits linear dichroism or birefringence. Rotational symmetry requires

$$K_{xx} = K_{yy}, \qquad K_{xy} = -K_{yx} \qquad (2)$$

for identical arguments $\mathbf{q}$, $\omega$, $\Delta$. One can then write the response to the circularly polarized EM waves, $\mathbf{A} = A_+\mathbf{e}_+ + A_-\mathbf{e}_-$ as $\mathbf{J} = J_+\mathbf{e}_+ + J_-\mathbf{e}_-$, with $\mathbf{e}_\pm = (\hat{x} \pm i\hat{y})/\sqrt{2}$ and

$$J_\pm = -K_\pm A_\pm \qquad (3)$$

$$K_\pm = K_{xx} \pm iK_{xy} \qquad (4)$$

The following relations are readily derived by considering the appropriate physical symmetry operations or by suitable manipulations of Eq. (1) or its Lehmann representation. We simply state the results:

(i) causality:

$$K_+(\mathbf{q}, \omega; \Delta)^* = K_-(-\mathbf{q}, -\omega; \Delta) \qquad (5)$$

(ii) $z \to -z$:

$$K_\pm(\mathbf{q}, \omega; \Delta) = K_\pm(-\mathbf{q}, \omega; \Delta^z) \qquad (6)$$

(iii) 2D parity ($x \to -x$ or $y \to -y$):

$$K_+(\mathbf{q}, \omega, \Delta) = K_-(\mathbf{q}, \omega; \Delta^P) \qquad (7)$$

(iv) time reversal:

$$K_{\pm}(\mathbf{q}, \omega; \Delta) = K_{\pm}(\mathbf{q}, -\omega; \Delta^*)^* \tag{8}$$

$$K_{+}(\mathbf{q}, \omega; \Delta) = K_{-}(-\mathbf{q}, \omega; \Delta^*) \tag{9}$$

Here $\Delta^z$ denotes the state obtained from $\Delta$ by the operation $z \to -z$ (in general $\Delta^z \neq \Delta$) and similarly for the 2D parity operation $P$. We also note that time-reversal converts $\Delta$ into $\Delta^*$ up to a gauge transformation. In general the time-reversed state should be $\sigma_y \Delta^* \sigma_y$; however, we shall confine ourselves to physical processes that are symmetric with respect to spin. Notice that Eqs. (8) and (9) are equivalent because of causality (Eq. (5)).

In addition to these fundamental symmetry relations, any good metal, and therefore essentially all known superconductors, possesses an approximate symmetry under the interchange of particle and hole excitations; i.e. particle–hole symmetry. This approximate symmetry is connected only with the low-energy excitations of the metallic state, and thus is violated if a physical process depends on excitations well away from the fermi surface. The magnitude of particle–hole asymmetry in metals is dimensionally of order $(k_B T_c/E_f)$ or $(\hbar\omega/E_f)$ compared with the low-energy contribution to a particular thermodynamic or transport coefficient. Particle–hole asymmetry corrections to the low-energy Fermi-liquid properties are essential if the leading order contribution from the low-energy excitations vanishes for symmetry reasons. This occurs, for example, in the thermoelectric coefficients of simple metals. In superfluids and superconductors particle–hole asymmetry is typically irrelevant, and essentially all know properties of superconductors and superfluid $^3$He can be accounted for by assuming perfect particle–hole symmetry. Superfluid $^3$He provides a few important exceptions. Basically, particle–hole asymmetry is important whenever it is associated with a coupling between excitations that are otherwise forbidden by selection rules. The most spectacular case is the observation of the $J=2^+$ collective mode in superfluid $^3$He-B, which is forbidden by particle–hole symmetry from coupling to either density or current fluctuations, but is observed as a sharp resonant absorption line in the zero-sound attenuation, albeit with a strength determined by the small particle–hole asymmetry factor $(k_B T_c/E_f)$ (see the reviews in Refs. 26 and 27). As we show below, for the superconducting state to exhibit circular dichroism and/or birefringence it is essential to consider the role of particle–hole asymmetry in the current response of the superconductor.

Under the particle–hole transformation, a particle above the Fermi surface is interchanged with a hole an equal distance below the Fermi surface (see, for example, Refs. 28 and 29). This transformation changes the sign of

the particle current, transforms $\Delta$ into $\Delta^*$ (more precisely $\sigma_y\Delta^*\sigma_y$ as in time reversal) and requires

$$K_\pm(\mathbf{q}, \omega; \Delta) = K_\pm(\mathbf{q}, \omega; \Delta^*) \tag{10}$$

if particle–hole symmetry is exact.

We can now discuss the necessary conditions for the observation of circular dichroism or birefringence in the reflectivity. For this it is necessary, but not sufficient (see Sec. 4), that $K_+(\mathbf{q}, \omega; \Delta) \neq K_-(\mathbf{q}, \omega; \Delta)$. We see from Eq. (7) that the breaking of 2D parity is necessary. However, time-reversal symmetry (i.e. $\Delta = \Delta^*$) by itself does not forbid the effect. But, if one also has reflection symmetry under $z \to -z$ (i.e. $\Delta = \Delta^z$), or when the physical process does not distinguish the sign of $\mathbf{q}$, then the effect would be forbidden (cf. the discussion of the zero-field Hall effect by Halperin *et al.*[19]). Approximate particle–hole symmetry puts a stringent constraint on the observability of circular dichroism. Perfect particle–hole symmetry implies that the response of the system is identical to that of its time-reversed state. Combined with Eqs. (9) and (6), particle–hole symmetry implies

$$K_+(\mathbf{q}, \omega; \Delta) = K_-(-\mathbf{q}, \omega; \Delta) = K_-(\mathbf{q}, \omega; \Delta^z) \tag{11}$$

Thus, if $\Delta = \Delta^z$, or when one is interested in an experiment that is insensitive to the sign of $\mathbf{q}$, then there is no circular dichroism or birefringence.

Note that Eq. (11) suggests a possible role of the surface in providing a mechanism for circular dichroism and birefringence; namely, surface scattering acts as a depairing mechanism which suppresses, or deforms, the order parameter $\Delta$ in the surface layer of order $\xi$. Surface depairing destroys the symmetry $\Delta = \Delta^z$ that may be obeyed for the bulk order parameter. Thus, it is possible that surface depairing will provide a contribution to circular dichroism from the surface layer of perturbed order parameter. We shall, however, not pursue this possibility here, but rather consider only the contributions to circular dichroism from the region of bulk order parameter, i.e. the layer of thickness $\xi < d \lesssim \lambda_L$.

We show in the next section that the response of the Bogoliubov quasiparticles is particle–hole symmetric (except for the trivial asymmetric terms referred to previously). The response due to collective modes of the order parameter in general does have non-trivial particle–hole asymmetric contributions, thus the circular dichroism or birefringence is due entirely to the difference in the collective mode response to $A_+$ and $A_-$; hence, one expects a strong dependence of the circular dichroism on the frequency. Combining Eq. (8) and Eq. (10) gives

$$K_\pm(\mathbf{q}, \omega; \Delta) = K_\pm(\mathbf{q}, -\omega; \Delta)^* \tag{12}$$

which shows that the nontrivial particle–hole asymmetry terms are also those which are asymmetric under $\omega \to -\omega$ together with complex conjugation. We now show how Eq. (12) manifests itself in the microscopic calculation.

## 3. MICROSCOPIC CALCULATION

We assume an order parameter of the Anderson–Brinkman–Morel (ABM) form, the orbital part of which is given by

$$\Delta(\hat{p}) = \Delta(T)(p_x + ip_y) \tag{13}$$

or $\Delta(p_x - ip_y)$ for its time-reversed state. This choice is representative of the class of superconducting states which break both time-reversal symmetry and 2D parity, but are rotationally invariant about the $\hat{z}$ axis under at least three-fold rotations. Other order parameters exhibiting these properties are, $\Delta \sim p_z(p_x \pm ip_y)(\Delta \sim \hat{z}(p_x \pm ip_y))$ and $\Delta \sim (p_x \pm ip_y)^2((\hat{x} \pm i\hat{y})(p_x \pm ip_y))$, which belong to the 2D representations $E_{1g(u)}$ and $E_{2g(u)}$, respectively. All of these order parameters have been discussed extensively as possible ground states of the heavy fermion superconductors $UPt_3$, $UBe_{13}$, $URu_2Si_2$, and to some extent the oxide superconductors.[3,5] Since these states exhibit the broken symmetries required for circular dichroism and birefringence, we expect the calculation presented for the ABM state to be qualitatively correct for this class of unconventional order parameters.

We also confine the discussion to clean superconductors, i.e. mean-free path $l \gg \xi$. Strong impurity scattering ($1/\tau_{\text{imp}} \gg \pi T_c$) will destroy an unconventional superconductor making this analysis irrelevant, while weak impurity scattering is expected only to modify the quantitative details of our calculation by broadening the collective modes.

To determine the reflection coefficient for EM waves incident on a superconductor we need a theory for the dynamics of the Bogoliubov quasiparticles as well as the condensate of Cooper pairs. We start from the formulation originally developed by Eilenberger,[30,31] Larkin and Ovchinnikov.[32] This quasiclassical theory is particularly well suited for calculating the EM response since "vertex corrections", which are closely related to the collective modes of the system, are included without special consideration. This theory has been further developed in the context of superfluid $^3$He and unconventional superconductors; we follow the notation of Serene and Rainer.[33]

The quasiclassical transport theory is formulated in terms of a $4 \times 4$ matrix propagator in particle–hole and spin space. In $2 \times 2$ particle–hole space $\hat{g}$ has the form

$$\hat{g}(\hat{p}, \varepsilon; \mathbf{q}, \omega) = \begin{pmatrix} g & f \\ \bar{f} & \bar{g} \end{pmatrix} \tag{14}$$

where each entry is a $2\times 2$ spin matrix. The diagonal functions are closely related to the distribution function for the Bogoliubov quasiparticles, while the off-diagonal functions are the Cooper pair amplitudes.

Since we are interested specifically in the reflectivity of unconventional superconductors with broken T- and P-symmetries we make the following simplifications of the full quasiclassical transport equation: (i) we neglect impurity-scattering, (ii) we consider only weak-coupling superconductors and neglect inelastic processes from both phonons and quasiparticle scattering—this amounts to retaining only the leading order mean-field self-energy, (iii) we assume an isotropic metal with a spherical Fermi surface, and finally, (iv) we calculate only the linear response of the superconductor to an incident EM wave. None of these simplifications are particularly restrictive for the problem of interest; however, there may be nonlinear parametric effects that are closely associated with broken time-reversal symmetry, broken parity and the observability of circular dichroism and birefringence.

For the linear response in the weak-coupling limit the matrix propagator satisfies the transport equation,

$$(\varepsilon+\omega/2)\hat{\tau}_3\delta\hat{g}-\delta\hat{g}(\varepsilon-\omega/2)\hat{\tau}_3+iv_f(\hat{p})\cdot\nabla\delta\hat{g}+\delta\hat{g}\hat{\Delta}-\hat{\Delta}\delta\hat{g}$$
$$+\hat{g}_{\rm eq}(\varepsilon+\omega/2)[\hat{\varepsilon}+\delta\hat{\Delta}]-[\hat{\varepsilon}+\delta\hat{\Delta}]\hat{g}_{\rm eq}(\varepsilon-\omega/2)=0 \tag{15}$$

where $\hat{\Delta}(\hat{p})$ is the mean-field, equilibrium order parameter, $\hat{\varepsilon}$ is the sum of the external field and the Landau mean field, and $\delta\hat{\Delta}$ is the time-dependent fluctuation of the order parameter that is driven by the EM field.

Since we are interested only in the response to transverse EM waves we can choose a gauge in which the scalar potential is zero and the vector potential satisfies $\mathbf{q}\cdot\mathbf{A}=0$; in this case the external field is given by

$$\hat{\varepsilon}(\hat{p};\mathbf{q},\omega)=\frac{e}{c}\mathbf{v}_f(\hat{p})\cdot\mathbf{A}\hat{\tau}_3 \tag{16}$$

There are also Fermi-liquid corrections to the external field; however, we ignore these effects here. But it should be kept in mind that Fermi-liquid corrections may be important, particularly if one is interested in the current response of heavy fermion superconductors.

The matrix form the order parameter field in particle–hole space is given by,

$$\hat{\Delta}=\begin{pmatrix}0 & \Delta\\ \bar{\Delta} & 0\end{pmatrix} \tag{17}$$

where $\bar{\Delta}(\hat{p}) = -\Delta(\hat{p})^{\dagger}$. There is redundancy of information contained in the matrix propagator, which is reflected in the symmetry relations,

$$\bar{g} = g(-\hat{p}, -\varepsilon; \mathbf{q}, \omega)^{\mathrm{tr}}, \qquad \bar{f} = -f(-\hat{p}, -\varepsilon; -\mathbf{q}, -\omega)^{*} \tag{18}$$

which follow from the definition of the propagators in terms of two-point Green's functions.[33]

The input to the linearized transport equation is the equilibrium propagator

$$\hat{g}_{\mathrm{eq}}(\hat{p}, \varepsilon) = \alpha(\hat{p}, \varepsilon)\hat{\tau}_3 + \beta(\hat{p}, \varepsilon)\hat{\Delta}(\hat{p}) \tag{19}$$

where

$$\alpha = -\varepsilon\beta = -2\pi i N(\hat{p}, \varepsilon) \tanh(\varepsilon/2T) \tag{20}$$

$$N(\hat{p}, \varepsilon) = \frac{|\varepsilon|}{\sqrt{\varepsilon^2 - |\Delta(\hat{p})|^2}} \Theta(\varepsilon^2 - |\Delta(\hat{p})|^2) \tag{21}$$

The equilibrium propagator contains information about the spectrum of single particle excitations ($N(\hat{p}, \varepsilon)$), the thermal distribution of these excitations ($\tanh(\varepsilon/2T)$), as well as the equilibrium order parameter ($\hat{\Delta}$). This latter quantity is determined self-consistently from the weak-coupling gap equation

$$\Delta(\hat{p}) = \int \frac{d\Omega'}{4\pi} V'(\hat{p} \cdot \hat{p}') \int_{-\varpi_c}^{\varpi_c} \frac{d\varepsilon}{4\pi i} \beta(\hat{p}', \varepsilon)\Delta(\hat{p}') \tag{22}$$

The diagonal and off-diagonal components of the matrix propagator are each $2 \times 2$ spin matrices. In order to solve the linear transport equation it is useful to expand the diagonal propagators in scalar and vector components,

$$\delta g = \delta g_s \sigma_0 + \delta \mathbf{g} \cdot \boldsymbol{\sigma}, \qquad \delta \bar{g} = \delta g_s' \sigma_0 + \delta \mathbf{g}' \cdot \boldsymbol{\sigma}^{\mathrm{tr}} \tag{23}$$

and the off-diagonal propagators in terms of spin-singlet and spin-triplet amplitudes,

$$\delta f = \delta f_0 i\sigma_2 + \delta \mathbf{f} \cdot i\boldsymbol{\sigma}\sigma_2, \qquad \delta \bar{f} = \delta f_0' i\sigma_2 + \delta \mathbf{f}' \cdot i\sigma_2\boldsymbol{\sigma} \tag{24}$$

We make a similar expansion of the time-dependent order parameter,

$$\delta\Delta = d_0 i\sigma_2 + \mathbf{d} \cdot i\boldsymbol{\sigma}\sigma_2, \qquad \delta\bar{\Delta} = d_0' i\sigma_2 + \mathbf{d}' \cdot i\sigma_2\boldsymbol{\sigma} \tag{25}$$

The mean-field self-consistency equations for the time-dependent order parameters are

$$d_0(\hat{p};\mathbf{q},\omega)=\int\frac{d\Omega'}{4\pi}\int_{-\varpi_c}^{\varpi_c}\frac{d\varepsilon}{4\pi i}V^s(\hat{p}\cdot\hat{p}')\delta f_0(\hat{p}',\varepsilon;\mathbf{q},\omega) \tag{26}$$

$$\mathbf{d}(\hat{p};\mathbf{q},\omega)=\int\frac{d\Omega'}{4\pi}\int_{-\varpi_c}^{\varpi_c}\frac{d\varepsilon}{4\pi i}V^t(\hat{p}\cdot\hat{p}')\delta\mathbf{f}(\hat{p}',\varepsilon;\mathbf{q},\omega) \tag{27}$$

Since we consider here only spin-triplet, $p$-wave pairing in the context of the ABM state, the self-consistency equation is considerably simplified by assuming only the triplet, $l=1$ pairing channel is relevant, i.e. $V^s=0$ and

$$V^t=3V_1\hat{p}\cdot\hat{p}'=3V_1[y_0(\hat{p})y_0(\hat{p}')^*+y_+(\hat{p})y_+(\hat{p}')^*+y_-(\hat{p})y_-(\hat{p}')^*] \tag{28}$$

where $y_m(\hat{p})$ are the spherical harmonics,

$$y_0=p_z,\qquad y_\pm=(p_x\pm ip_y)/\sqrt{2} \tag{29}$$

normalized to

$$\int\frac{d\Omega}{4\pi}y_m(\hat{p})^*y_{m'}(\hat{p})=\tfrac{1}{3}\delta_{m,m'} \tag{30}$$

Although the ABM state is a spin-triplet condensate, the electromagnetic properties we consider here are independent of the spin structure of the order parameter and depend only on the broken time-reversal and 2D parity symmetries of the orbital part of the order parameter. Thus, only the scalar component of the diagonal propagator, and the components of the order parameter which couple to these scalars are relevant.

In terms of the functions $\alpha$, $\beta$ and the equilibrium order parameter, the relevant linearized transport equations become,

$$\begin{pmatrix}-\eta & \omega & 2i\Delta_I & -2\Delta_R\\ \omega & -\eta & 0 & 0\\ 2i\Delta_I & 0 & -\eta & 2\varepsilon\\ 2\Delta_R & 0 & 2\varepsilon & -\eta\end{pmatrix}\begin{pmatrix}\delta g^-\\ \delta g^+\\ \delta f_L^+\\ \delta f_L^-\end{pmatrix}$$

$$=-\begin{pmatrix}0 & D_\alpha & -iS_\beta\Delta_I & S_\beta\Delta_R\\ D_\alpha & 0 & -D_\beta\Delta_R & iD_\beta\Delta_I\\ -iS_\beta\Delta_I & D_\beta\Delta_R & 0 & S_\alpha\\ -S_\beta\Delta_R & iD_\beta\Delta_I & S_\alpha & 0\end{pmatrix}\begin{pmatrix}\varepsilon^-\\ \varepsilon^+\\ d_L^+\\ d_L^-\end{pmatrix} \tag{31}$$

where $\eta = \mathbf{q} \cdot \mathbf{v}_f(\hat{p}) = q_z v_f p_z$, and $\Delta_{R(I)}$ is the real (imaginary) part of the equilibrium order parameter. The matrix elements $D_{\alpha(\beta)}$ and $S_{\alpha(\beta)}$ are given in Appendix I, while the $\pm$ functions are defined by $B^{\pm} = B \pm B'$. The subscript $L$ refers to the "longitudinal" component of the time-dependent pair amplitude, i.e.

$$\delta f_L^{\pm} = (\delta \mathbf{f}^{\pm} \cdot \hat{d})\hat{d}\,, \tag{32}$$

where $\hat{d}$ is a unit vector defining the spin quantization axis of the ABM phase order parameter,

$$\Delta_{\mathrm{ABM}} = \hat{d}\Delta(T)(p_x + ip_y) \tag{33}$$

The ABM pairs have spin projection $\hat{d} \cdot \mathbf{S} = 0$. The $\pm$ functions are introduced in order to block diagonalize the full linear transport equation. These linear combinations are also important because they obey simple relations under $\varepsilon \to -\varepsilon$ and $\hat{p} \to -\hat{p}$; e.g. $\delta g^{\pm}(\hat{p}, \varepsilon) \to \pm \delta g^{\pm}(-\hat{p}, -\varepsilon)$. We can similarly define the transverse component of the pair amplitude,

$$\delta \mathbf{f}_T^{\pm} = \delta \mathbf{f}^{\pm} - \delta \mathbf{f}_L^{\pm} \tag{34}$$

These transverse amplitudes, which are needed to construct the full time-dependent gap equation, satisfy the same matrix equation, except that the column vectors, $|g_L\rangle$ and $|\varepsilon_L\rangle$, respectively, in Eq. (31) are replaced by

$$|g_T\rangle = \begin{pmatrix} \delta \mathbf{g}_{T'}^{-} \\ \delta \mathbf{g}_{T'}^{+} \\ i\delta \mathbf{f}_T^{-} \\ i\delta \mathbf{f}_T^{+} \end{pmatrix} \quad \text{and} \quad |\varepsilon_T\rangle = \begin{pmatrix} 0 \\ 0 \\ i\mathbf{d}_T^{-} \\ i\mathbf{d}_T^{+} \end{pmatrix} \tag{35}$$

where $\mathbf{B}_{T'} = \hat{d} \times \mathbf{B}_T$. The solution of Eq. (31) yields the linear response functions in terms of the external fields $\varepsilon^{\pm}$ and the fluctuations of the order parameter $\mathbf{d}^{\pm}$;

$$|g_{L(T)}\rangle = -\hat{m}(\hat{p}, \varepsilon; \mathbf{q}, \omega)|\varepsilon_{L(T)}\rangle \tag{36}$$

where the matrix elements of $\hat{m}(\hat{p}, \varepsilon; \mathbf{q}, \omega)$ are given in Appendix I.

Since the order parameter and mean-fields are independent of the excitation energy, $\varepsilon$, the standard procedure is to $\varepsilon$-integrate Eq. (36), in which case we need only calculate the equal-time functions,

$$\delta \check{g}^{\pm} = \int \frac{d\varepsilon}{2\pi i} \delta g^{\pm}(\hat{p}, \varepsilon; \mathbf{q}, \omega) \tag{37}$$

$$\delta \check{\mathbf{f}}^{\pm} = \int \frac{d\varepsilon}{2\pi i} \delta \mathbf{f}^{\pm}(\hat{p}, \varepsilon; \mathbf{q}, \omega) \tag{38}$$

However, direct integration of the quasiclassical propagator implicitly assumes exact particle–hole symmetry. This is clear from inspection of the solution of the linear transport equation (see Appendix I); the matrix elements involve terms that are explicitly even or odd under $\varepsilon \to -\varepsilon$. Odd contributions, i.e. terms which are odd under the particle–hole transformation, vanish when integrated. Particle–hole asymmetry contributions to the response functions are included by noting that quantities like the quasiparticle density of states, Fermi velocity, pairing interaction, *etc.*, vary weakly with excitation energy away from the Fermi surface. Since the typical energy scale for this variation is the Fermi energy, this weak energy dependence is of little consequence for processes that are determined by excitations near the Fermi surface. However, certain properties, in particle circular dichroism and birefringence, vanish when these high-energy contributions are neglected; i.e. particle–hole symmetry, combined with the symmetry $z \to -z$, provides a selection rule prohibiting these effects. Thus, we retain the particle–hole asymmetric contributions to the propagators. An expansion of the density of states near the Fermi surface leads to corrections to the particle–hole symmetric equal-time propagators of the form

$$\delta\check{g}^{\pm} = \int \frac{d\varepsilon}{2\pi i}\left(1 + a\frac{\varepsilon}{E_f}\right)\delta g^{\pm}(\hat{p}, \varepsilon; \mathbf{q}, \omega) \tag{39}$$

where $a$ is a material parameter of order one. Most importantly, the current response is given by

$$\mathbf{j}(\mathbf{q}, \omega) = -eN(E_f)\int \frac{d\Omega}{4\pi}\mathbf{v}_f(\hat{p})\delta\check{g}(\hat{p}; \mathbf{q}, \omega) \tag{40}$$

where the scalar part of the equal-time propagator, including particle–hole asymmetry terms, is given by $\delta\check{g} = (\delta\check{g}^{+} + \delta\check{g}^{-})/2$. Similar expressions for the equal-time, off-diagonal propagators hold. The time-dependent gap equations, including particle–hole asymmetry terms, are then given by

$$\mathbf{d}^{\pm}(\hat{p}; \mathbf{q}, \omega) = \frac{1}{2}\int \frac{d\Omega'}{4\pi} V'(\hat{p}\cdot\hat{p}')\delta\check{\mathbf{f}}^{\pm}(\hat{p}'; \mathbf{q}, \omega) \tag{41}$$

Inspection of the matrix solutions to the scalar equations for $\delta\check{g}^{\pm}$ and the related order parameter response shows that, although there are particle–hole asymmetry corrections to $\delta\check{g}^{-}$, they do not contribute to circular dichroism or birefringence. However, the contributions to the transverse current from $\delta\check{g}^{+}$ are only non-zero because of particle–hole asymmetry. Most importantly these terms provide the entire contribution to the circular dichroism.

The solutions for the scalar propagators are

$$\delta\check{g}^{-}(\hat{p};\mathbf{q},\omega)=2\left[1+\left(\frac{\eta^2}{\omega^2-\eta^2}\right)(1-\lambda)\right]\left(\frac{2e}{c}\mathbf{v}_f(\hat{p})\cdot\mathbf{A}\right)$$
$$+\eta\bar{\lambda}(\boldsymbol{\Delta}_R\cdot\mathbf{d}^{-}-i\boldsymbol{\Delta}_I\cdot\mathbf{d}^{+})$$
$$+\frac{\omega}{\omega^2-\eta^2}\mu^{-}(\omega)(\boldsymbol{\Delta}_R\cdot\mathbf{d}^{+}-i\boldsymbol{\Delta}_I\cdot\mathbf{d}^{-}) \tag{42}$$

$$\delta\check{g}^{+}(\hat{p};\mathbf{q},\omega)=2\left[\left(\frac{\eta\omega}{\omega^2-\eta^2}\right)(1-\lambda)\right]\left(\frac{2e}{c}\mathbf{v}_f(\hat{p})\cdot\mathbf{A}\right)$$
$$+\omega\bar{\lambda}(\boldsymbol{\Delta}_R\cdot\mathbf{d}^{-}-i\boldsymbol{\Delta}_I\cdot\mathbf{d}^{+})$$
$$+\frac{\eta}{\omega^2-\eta^2}\mu^{+}(\omega)(\boldsymbol{\Delta}_R\cdot\mathbf{d}^{+}-i\boldsymbol{\Delta}_I\cdot\mathbf{d}^{-}) \tag{43}$$

where the function $\lambda(\hat{p};\mathbf{q},\omega)=|\Delta(\hat{p})|^2\bar{\lambda}$ is the Tsuneto function (defined in the Appendix I) and $\mu^{\pm}(\omega)$ are particle–hole asymmetry response functions, which are typically of order

$$\mu^{\pm}\sim\left(\frac{\Delta}{E_f}\right)\ln\left(\frac{\varpi_c}{\Delta}\right) \tag{44}$$

compared with the particle–hole symmetric terms of order $\lambda\sim 1$. Note that the particle–hole asymmetry terms are cutoff-dependent, reflecting their origin as high-energy corrections to the low-energy response functions. While we do not give a systematic discussion of the leading order high-energy corrections to the low-energy response, the important contributions to the current response can be parametrized by a small number of particle–hole asymmetry response functions.

An important feature of the scalar solutions is that the coupling of the current to the order parameter is determined entirely by the orbital response of the order parameter, i.e. $d^{\pm}=\hat{d}\cdot\mathbf{d}^{\pm}$. The equations for the spin-independent order parameter fluctuations, $d$ and $d'$, are easily obtained from Eq. (36),

$$d(\hat{p})=\frac{1}{2}\int\frac{d\Omega'}{4\pi}V'(\hat{p}\cdot\hat{p}')\left\{-\tfrac{1}{2}(\eta'\bar{\lambda}+\tilde{\mu})\Delta(\hat{p}')\left[\frac{2e}{c}\mathbf{v}_f(\hat{p}')\cdot\mathbf{A}\right]\right.$$
$$+[\gamma(\hat{p}')+\tfrac{1}{2}(\omega^2-\eta'^2)\bar{\lambda}]d(\hat{p}')$$
$$\left.-\bar{\lambda}[|\Delta(\hat{p}')|^2d(\hat{p}')+\Delta(\hat{p}')^2d'(\hat{p}')]\right\}, \tag{45}$$

$$d'(\hat{p}) = \frac{1}{2}\int \frac{d\Omega'}{4\pi} V^t(\hat{p}\cdot\hat{p}')\left\{\tfrac{1}{2}(\eta'\bar{\lambda}-\tilde{\mu})\Delta^*(\hat{p}')\left[\frac{2e}{c}\mathbf{v}_f(\hat{p}')\cdot\mathbf{A}\right]\right.$$
$$+[\gamma(\hat{p}')+\tfrac{1}{2}(\omega^2-\eta'^2)\bar{\lambda}]d'(\hat{p}')$$
$$\left.-\bar{\lambda}[|\Delta(\hat{p}')|^2 d'(\hat{p}')+\Delta^*(\hat{p}')^2 d(\hat{p}')]\right\}. \tag{46}$$

where $\tilde{\mu}=\omega\mu^-/(\omega^2-\eta'^2)$. These are inhomogeneous integral equations for the order parameter response; note that both the real and imaginary parts of the order parameter are excited by the field.

The solutions to the homogeneous equations for $d(\hat{p})$ and $d'(\hat{p})$ determine the collective modes of the ABM phase, rather the spin-independent collective modes. These modes have been studied extensively in the context of superfluid $^3$He (cf. Wölfle[34,35] and Halperin[27]).

Assume that the ground state order parameter is the ABM state with $m=+1$,

$$\Delta(\hat{p}) = \sqrt{2}\,\Delta(T) y_+(\hat{p}) \tag{47}$$

The collective modes are then given in terms of the amplitudes

$$d_m = 3\int \frac{d\Omega}{4\pi} y_m^*(\hat{p}) d(\hat{p}) \tag{48}$$

and similarly for $d'_m$. In particular the modes with $m=0$, the "flapping modes" of $^3$He-A, are important for the EM response. Both $d_0$ and $d'_0$ obey the same homogeneous equation; the collective mode frequency is determined by the transcendental equation,

$$\frac{\omega_0^2}{2\Delta(T)^2} = \frac{1}{\lambda_{00}}(\gamma_1-\gamma_0)+\left(1-\frac{\lambda_{20}}{\lambda_{00}}\right)+\frac{q_z^2 v_f^2}{2\Delta(T)^2}\frac{\lambda_{20}}{\lambda_{00}} \tag{49}$$

where the functions $\lambda_{nm}$ and $\gamma_m$ are defined in Appendix I. There are in fact multiple solutions to this equation; a low frequency mode called the "normal flapping mode", with $\omega_{\rm nfl}\simeq(T/T_c)\Delta(T)$ for $T\to 0$, and a high-frequency mode termed the "superflapping mode" with $\omega_{\rm sfl}\simeq 1.56\Delta(T)$ for $T\to 0$. The flapping modes are not sharp excitations. The excitation frequencies are in fact the solutions only to the real part of Eq. (49); the imaginary part of Eq. (49) is typically small, but non-zero, at these frequencies. As a consequence the flapping modes are resonances rather than sharp collective excitations because the continuum of single-particle excitations that exists in the ABM state gives rise to pair-breaking at any temperature and frequency. The effective width of these resonances is, however, small except near $T_c$.

The excitation of the order parameter by the EM field is easily obtained by expanding the order parameter in terms of the eigenmodes,

$$d(\hat{p}) = \sum_m d_m(\omega) y_m(\hat{p}) \tag{50}$$

and similarly for $d'$. By inserting this expansion into Eqs. (45) and (46) it is easy to see that only the $m=0$ modes are excited by a transverse field,

$$d_0(q_z, \omega) = \sqrt{2}\left(\frac{q_z v_f}{\Delta(T)}\right)\left(\frac{e}{c}\right) R(\omega) A_- \tag{51}$$

$$d_0'(q_z, \omega) = -\sqrt{2}\left(\frac{q_z v_f}{\Delta(T)}\right)\left(\frac{e}{c}\right) R(\omega) A_+ \tag{52}$$

where the frequency dependence of the function $R(\omega)$ is determined primarily by the flapping modes,

$$R(q_z, \omega) = \frac{\lambda_{21}}{(\omega^2/2\Delta^2)\lambda_{00} - [(\gamma_1 - \gamma_0) + (q_z^2 v_f^2/2\Delta^2)\lambda_{20} + (\lambda_{00} - \lambda_{20})]} \tag{53}$$

The electromagnetic response function can now be calculated. The contributions are from the Bogoliubov excitations, and the $m=0$ collective modes, so the response functions for the circularly polarized amplitudes can be written

$$K_\pm = K^{\text{ex}} + K_s^{\text{mode}} \pm K_a^{\text{mode}} \tag{54}$$

The contribution from the excitations is obtained from Eq. (42),

$$K^{\text{ex}} = \tfrac{3}{2} K_0 \int \frac{d\Omega}{4\pi} (1 - p_z^2) \left\{ 1 + \left( \frac{q_z^2 v_f^2 p_z^2}{\omega^2 - q_z^2 v_f^2 p_z^2} \right) (1 - \lambda(\hat{p}; q_z, \omega)) \right\} \tag{55}$$

where $K_0 = \frac{3}{2}(e^2/c) N(E_f) v_f^2$ determines the Meissner current in the static, long wavelength limit. In particular, the zero-temperature London screening length is given by $1/\lambda_0^2 = 4\pi K_0/c$. Note that the first term in Eq. (55) is simply the pure diamagnetic response of the metal.

There are two collective mode contributions to the EM kernel; the particle–hole symmetric contribution (from Eq. (42))

$$K_s^{\text{mode}} = K_0 \left( \frac{q_z v_f}{\Delta(T)} \right)^2 \lambda_{21} R(\omega) \tag{56}$$

which does not produce circular dichroism or birefringence, and the particle–hole asymmetric term (from Eq. (43))

$$K_a^{\text{mode}} = K_0 \left( \frac{q_z v_f}{\omega} \right)^2 \mu^+(\omega) R(\omega) \tag{57}$$

which determines the magnitude and frequency dependence of the circular dichroism and birefringence.

## 4. REFLECTION OF POLARIZED RADIATION

From the current response we are now able to calculate the reflection coefficient of an incident EM wave, and in particular the change in polarization of the reflected radiation. The analysis is similar to that of Ref. 36 for the absorption of radiation from collective modes for an unconventional superconductor in the Balian–Werthamer state. Consider a linearly polarized beam normally incident along the $\hat{z}$ axis of crystal. The two circularly polarized components are in general reflected with different amplitudes and phases, and hence the reflected beam is elliptically polarized.

In order to calculate the reflection amplitude for light incident from vacuum ($z<0$) we first need to solve the half-space boundary value problem in terms of the electromagnetic response function $K_\pm(\mathbf{q}, \omega)$ calculated for a bulk superconductor. This requires a boundary condition for the electromagnetic field and current at $z=0$. The half-space boundary-value problem is mapped onto the full space by assuming specular boundary conditions at the vacuum/metal interface. The kernel relating the current at point $\mathbf{r}_1$ to the vector potential at another point $\mathbf{r}_2$ is the sum of a direct contribution from $\mathbf{r}_2$ and an indirect contribution from the image of $\mathbf{r}_2$ due to specular reflection from the surface. Thus, we determine the physical vector potential by continuing the vector potential into the region $z<0$ by mirror reflection about $z=0$. The vector potential is then obtained by solving the Maxwell equation, with the mirror boundary condition and the constitutive Eq. (3), by Fourier transform,

$$\left( q_z^2 + \frac{4\pi}{c} \underline{K} \right) \cdot \mathbf{A} = -iq_z \operatorname{disc} \mathbf{A}(0) - \operatorname{disc} \frac{\partial \mathbf{A}}{\partial z}(0) \tag{58}$$

where the right side contains the discontinuities of the EM field at $z=0$ for the fictitous full-space problem. In particular, the specular boundary condition gives, $\operatorname{disc} \mathbf{A}(0)=0$ and $\operatorname{disc} \partial\mathbf{A}/\partial z(0) = 2\, \partial\mathbf{A}/\partial z|_{z=0^+}$. We now match this solution for $z>0$ to the physical situation of an incident EM

wave from the vacuum side. Consider the circularly polarized incident wave,

$$\mathbf{A}_{\text{inc}}(z, t) = A_0(\mathbf{e}_- e^{i((\omega/c)z-\omega t)} + \text{c.c.}). \tag{59}$$

The corresponding reflected wave is parametrized by

$$\mathbf{A}_{\text{ref}}(z, t) = A_0(r_- \mathbf{e}_- e^{i(-(\omega/c)z-\omega t)} + \text{c.c.}) \tag{60}$$

where $r_-$ is a complex reflection coefficient specifying the amplitude and phase relative to the incident wave. The total vector potential in the half-space $z<0$ is $\mathbf{A}=\mathbf{A}_{\text{inc}}+\mathbf{A}_{\text{ref}}$, and since the tangential components of both the electric and magnetic fields are continuous at the half-space boundary we obtain the desired relation determining the reflection coefficient in terms of the current response of the superconductor from continuity of the vector potential and its $z$ derivative at the surface. Combining the last three equations we find that the spatially varying vector potential in the superconductor is given by

$$\int \frac{dq_z}{2\pi} A_0 \left[ -2i \frac{\omega}{c} \frac{1-r_-}{q_z^2 + (4\pi/c)K_-(q_z, \omega)} \mathbf{e}_- e^{i(q_z z-\omega t)} + \text{c.c.} \right] \tag{61}$$

Continuity of the vector potential at $z=0$ gives

$$1 + r_- = -2i \frac{\omega}{c} \int \frac{dq_z}{2\pi} \frac{1-r_-}{q_z^2 + (4\pi/c)K_-(q_z, \omega)} \tag{62}$$

In terms of the dimensionless integral

$$I_-(\omega) = -2 \frac{\omega}{c} \int \frac{dq_z}{2\pi} \frac{1}{q_z^2 + (4\pi/c)K_-(q_z, \omega)} \tag{63}$$

we obtain

$$r_- = -\frac{1 - iI_-}{1 + iI_-} \tag{64}$$

Clearly for an incident wave of the opposite circular polarization we simply replace $r_- \to r_+$, $I_- \to I_+$, with $K_- \to K_+$. Now the reflected wave of a linearly polarized wave is completely determined by the reflection coefficients $r_\pm$, or in terms of the Stokes parameters,

$$\tilde{S}_0 = \tfrac{1}{2}(|r_-|^2 + |r_+|^2) \tag{65}$$

$$\tilde{S}_1 = \text{Re}(r_-^* r_+) \tag{66}$$

$$\tilde{S}_2 = \text{Im}(r_-^* r_+) \tag{67}$$

$$\tilde{S}_3 = \tfrac{1}{2}(|r_-|^2 - |r_+|^2) \tag{68}$$

which specify the total reflected amplitude ($\tilde{S}_0$), relative phase and amplitude ($\tilde{S}_{1,2}$), and the difference in the amplitudes ($\tilde{S}_3$) of the two outgoing circularly polarized components.

In order to calculate these quantities the evaluation of the integrals $I_\pm$ is enormously simplified by noting that the typical values of the wavevector contributing to the integral are $q_z \sim \lambda_L^{-1}$ so that $q_z^2 v_f^2/\omega^2 \ll 1$ for relevant frequencies $\omega \gtrsim \Delta$; for $\omega = \Delta$ this ratio is already very small, of order $(\xi/\lambda_L)^2$. With this assumption the EM response function simplifies to

$$\frac{4\pi}{c} K_\pm(q_z, \omega) \simeq \frac{1}{\lambda_0^2}\left(1 + b_\pm(\omega)\frac{q_z^2 v_f^2}{\omega^2}\right) \tag{69}$$

The integral in Eq. (63) is simple to evaluate and gives

$$I_\pm = -\frac{\omega\lambda_0}{c}\frac{1}{\sqrt{1 + b_\pm(\omega)(v_f^2/\lambda_0^2\omega^2)}} \approx -\frac{\omega\lambda_0}{c}\left(1 - \tfrac{1}{2} b_\pm(\omega)\frac{v_f^2}{\lambda_0^2\omega^2}\right) \tag{70}$$

barring anomalously large values of the coefficient $b_\pm(\omega)$ (see below). Finally, the reflection coefficient is obtained to leading order in $(v_f/\lambda_0\omega)$,

$$r_\pm = -\frac{1 + i(\omega\lambda_0/c)}{1 - i(\omega\lambda_0/c)}\left(1 - i b_\pm(\omega)\frac{v_f/c(v_f\lambda_0/\omega)}{1 + (\omega\lambda_0/c)^2}\right) \tag{71}$$

The corresponding Stokes parameters can be written in terms of the dimensionless function $b_\pm(\omega)$ as

$$\tilde{S}_0 = \tilde{S}_1 = 1 + S_0 f(\omega), \qquad \tilde{S}_2 = S_2 f(\omega), \qquad \tilde{S}_3 = S_3 f(\omega) \tag{72}$$

where

$$f(\omega) = \frac{(v_f/c)(v_f/\lambda_0 T_c)}{1 + (\omega\lambda_0/c)^2} \tag{73}$$

$$\begin{aligned} S_0 &= \left(\frac{T_c}{\omega}\right)(\mathrm{Im}\, b_- + \mathrm{Im}\, b_+) \\ S_2 &= \left(\frac{T_c}{\omega}\right)(\mathrm{Re}\, b_- - \mathrm{Re}\, b_+) \\ S_3 &= \left(\frac{T_c}{\omega}\right)(\mathrm{Im}\, b_- - \mathrm{Im}\, b_+) \end{aligned} \tag{74}$$

Note that $c/\lambda_0 = \omega_p$ is the plasma frequency, so that for the materials we are interested in the relevant frequencies are small compared to $\omega_p$, and hence

$f(\omega)$ is essentially frequency independent and small, of order $10^{-5}$–$10^{-6}$ for both the heavy fermion and oxide superconductors.

From Eqs. (57), (72), (73), and (74) we can estimate the order of magnitude of the circular dichroism,

$$\tilde{S}_{2(3)} \sim \left(\frac{v_f}{c}\right)\left(\frac{\xi}{\lambda_0}\right)\left(\frac{\Delta}{\omega}\right)\left(\frac{\Delta}{E_f}\right)\ln\left(\frac{\tilde{\omega}_c}{\Delta}\right)R(\omega)$$

which for parameters appropriate for the high $T_c$ or heavy fermion superconductors is of order $10^{-7}$–$10^{-8}$ at frequencies $\omega \sim \Delta$.

Finally, we comment on the assumption made in evaluating the integral in Eq. (63), namely that $|b_\pm| v_f/\lambda_0 \omega \ll 1$. This is a good approximation provided that $|b_\pm| \ll \lambda_0/\xi$. This is not a priori obvious, particularly for frequencies near the flapping mode frequencies, since one can in principle have strong absorption of the EM field by the collective mode and consequently decay of the field on a length scale much shorter than the London length. If this were so the characteristic wavevectors contributing to the integral in Eq. (63) are much larger than $\lambda_0^{-1}$. However, because of the nodes in the equilibrium gap of the ABM phase there is pairbreaking at all temperatures and frequencies so that the resonant absorption from the collective mode is broadened, sufficiently so that the inequality $|b_\pm| \ll \lambda_0/\xi$ is not violated even for frequencies near the flapping mode resonance.

## 5. NUMERICAL RESULTS AND DISCUSSION

Before we discuss our results it is useful to review the properties of the flapping modes.[34,35,37] The collective mode frequency is defined as the solution to the real part of the denominator of Eq. (53). In fact there are two solutions at a fixed temperature. The low-frequency mode, known as the "normal flapping mode," has a frequency that is linear in temperature at low temperature, $\omega \sim T$, and is proportional to the maximum energy gap at higher temperatures, $\omega_{\text{nfl}} = \sqrt{4/5}\,\Delta(T)$ for $T \to T_c$. The high-frequency mode, known as the "superflapping mode," has a weaker temperature dependence of the frequency, $\omega_{\text{sfl}} \simeq 1.6\Delta$ for $T \ll T_c$ and $\omega_{\text{sfl}} \to 2\Delta(T)$ for $T \to T_c$. We emphasize that the imaginary part of the denominator is nonzero at these frequencies because pair-breaking exists at any temperature due to the nodes of the ABM gap. As a consequence the flapping modes are resonances rather than true collective modes.

We present the numerical results for the optical dichroism and birefringence for the model system with $E_f/T_c = 100$, $\tilde{\omega}_c/T_c = 10$. The gap parameter $\Delta(T)$ is represented by the interpolation formula given by Wöfle and Koch,[37] with a weak coupling value for the specific heat jump (which determines how

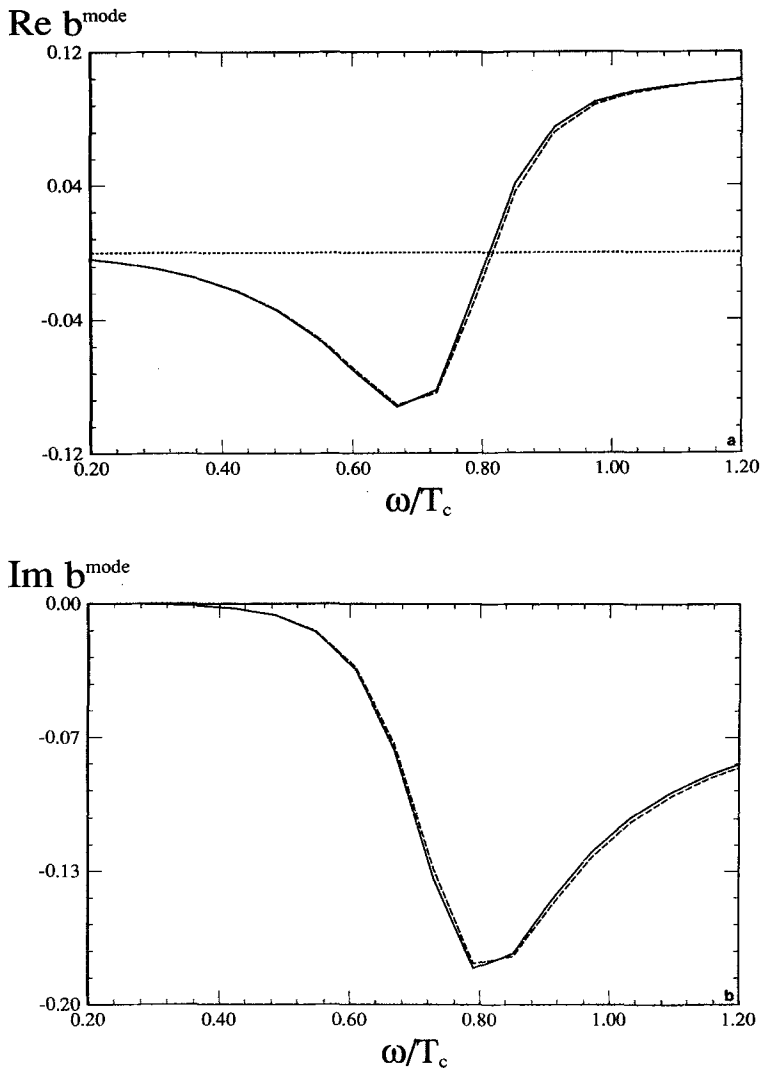


Fig. 1. The real and imaginary parts of $b_{\pm}$ of the collective mode response at $T/T_c = 0.5$ as functions of frequency $(\omega/T_c)$. Full curves and dashed curves are for $b_{-}^{\text{mode}}$ and $b_{+}^{\text{mode}}$ respectively. (a) $\text{Re}(b_{\pm})$; (b) $\text{Im}(b_{\pm})$.

fast the gap opens up as $T$ decreases below $T_c$). The asymmetry parameter $a$ is chosen to be 0.1. Since the (scaled) Stokes parameters $S_2$, $S_3$ arise from the difference of the response to the two circular polarizations, they are simply proportional to the particle–hole asymmetry parameter $a$, for

$a \ll E_F/\Delta$. The contributions to $S_0$ are mainly from particle–hole symmetric terms, and hence $S_0$ is roughly independent of $a$. The results are presented with frequencies in units of $T_c$.

In order to interpret the behavior of the Stokes parameters, we first show in Fig. 1 the behavior of the collective mode contributions to $\mathrm{Re}(b_\pm)$ and $\mathrm{Im}(b_\pm)$, for the temperature $T=0.5T_c$, and frequencies near the normal flapping mode frequency ($\omega \approx 0.8T_c$). The functions $\mathrm{Re}\, b_\pm^{\mathrm{mode}}$, $\mathrm{Im}\, b_\pm^{\mathrm{mode}}$ show the characteristic form of a resonance for the in-phase and out-of-phase components of the response, respectively. The effect of the particle–hole asymmetry is barely discernible as a horizontal displacement of the two curves $b_\pm^{\mathrm{mode}}$ for the two circular polarizations. Figure 2 shows the (scaled) Stokes parameters $S_0$, $S_2$, $S_3$ as functions of frequency at the same temperature. At this temperature, besides the normal flapping mode at $\omega \approx 0.4\Delta(T)$ ($\omega = 0.8T_c$) there is also the superflapping mode at $\omega = 1.65\Delta(T)$ ($\omega/T_c = 3.3$). At the normal flapping mode, $S_0$ has a strong negative dip, whereas $S_2$ goes from a negative maximum to a positive maximum and then goes negative again above the resonance. $S_3$ in turn has a negative and a positive maxima on the two sides of the resonance. This behavior is easily understood by inspecting Eq. (74) and the resonance behavior of $\mathrm{Re}\, b_\pm^{\mathrm{mode}}$, $\mathrm{Im}\, b_\pm^{\mathrm{mode}}$ above.

At higher frequency, $\omega \approx 3.3T_c$, near the superflapping mode, we do not see any significant features in any of the three Stokes parameters, though we checked that the real part of the denominator in Eq. (53) does vanish there.

This absence of any sharp feature near the superflapping mode is because of a significant imaginary part of the denominator, representing damping of the mode (pair-breaking and Landau damping by thermal excitations both increase strongly with frequency). This is similar to the case of sound attenuation in $^3$He–$A$, where the superflapping mode gives features much less significant than the normal flapping mode.

At even higher frequency, $\omega \approx 4T_c$, where $\omega = 2\Delta(T)$, we see that there are sudden changes in slope for $S_0$, $S_2$, $S_3$ (the latter two may be too difficult to see for the scales used in Fig. 2). These anomalies are due to sharp increases in pair-breaking for $\omega > 2\Delta(T)$. Thus, the response of the system follows a different frequency dependence for $\omega \gtrless 2\Delta(T)$, although there is no discontinuity of the response itself at $\omega = 2\Delta(T)$.

Figures 3 and 4 show the scaled Stokes parameters at fixed frequencies as functions of temperature. Figure 3 shows the typical case for a "low" frequency. At $\omega/T_c = 0.6$, the normal flapping mode has strong temperature dependence even when scaled by $\Delta(T)$; the frequency matches the collective mode frequency at two temperatures: $T/T_c \approx 0.35$ ($\omega \approx 0.28\Delta(T)$), and $T/T_c \approx 0.95$ ($\omega \approx 0.8\Delta(T)$). This "reentrant" behavior is well-known in the

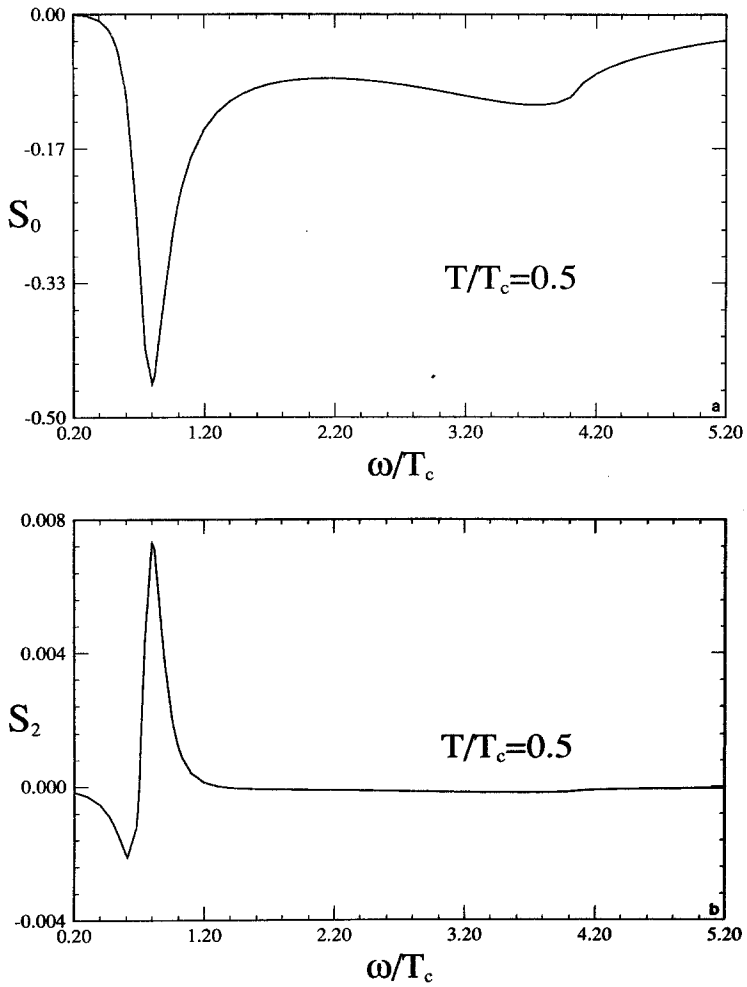


Fig. 2. The scaled Stokes parameters of Eq. (74) as functions of frequency $(\omega/T_c)$ at $T/T_c=0.5$. (a) $S_0$; (b) $S_2$; (c) $S_3$.

ultrasonic attentuation in $^3$He–$A$. The frequency also matches the superflapping mode and $2\Delta(T)$ at $T$ very close to $T_c$, but no observable feature can be seen for the scale used in Figs. 3 and 4.

Again $S_0(\omega)$ shows significant absorption near the normal flapping mode frequencies. The structure in $S_2$ and $S_3$ can be understood in terms of the resonance behavior of $b_{\pm}^{\text{mode}}$ as in Fig. 2. Note that $S_2$ and $S_3$ approach zero as $T\to T_c$, since the broken symmetry exists only in the presence of the order parameter.

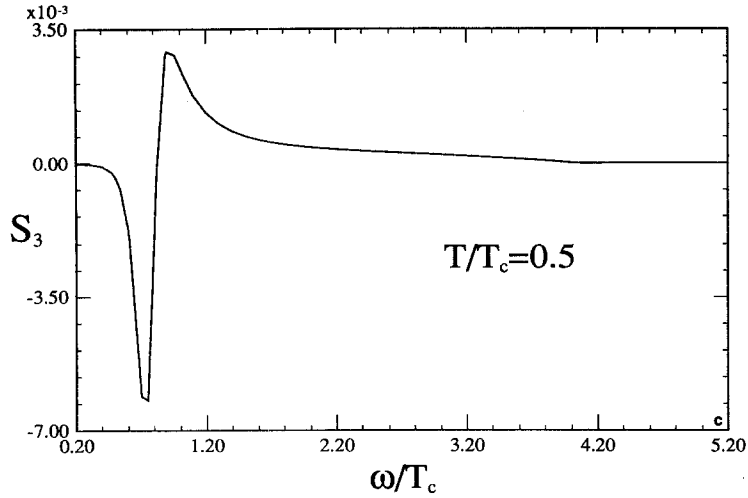


Fig. 2. Continued.

The typical "high frequency" behavior is shown in Fig. 4 (note the difference in scale from Fig. 2). At $\omega = 3.0T_c$ the frequency does not match the normal flapping mode. The frequency does match the superflapping mode at $T \approx 0.71T_c$, but again no significant feature can be resolved. At $T \approx 0.8T_c$, however, $\omega = 2\Delta(T)$, where we expect changes in slopes of the Stokes parameters as functions of temperature. We can see this rapid change for $S_0$ and $S_2$ (notice that there is no change of sign), however, the behavior of $S_3$ is much more dramatic. It has a sharp dip near $T \approx 0.8T_c$, reaching a very small, but nonzero value. By increasing the particle–hole asymmetry parameter from the present value of 0.1, we can smooth out this dip and, in fact, at $a \approx 4$ the slope on the high temperature side changes from positive to negative, and the dip evolves into a simple kink, where the magnitude of the (negative) slopes decreases suddenly.

We now briefly comment on the experimental searches for circular dichroism and birefringence in light of our calculations. Lyons *et al.*[21] reported a nonzero signal for circular dichroism or birefringence well above $T_c$ for $Ba_2YCu_3O_7$ and $Bi_2Sr_2CaCu_2O_8$. However, no change across $T_c$ was observed. Thus, their signal is unlikely to be related to superconductivity. In their second experiment[22] on $Rb_xBa_{1-x}BiO_3$ as well as the experiment on YBaCuO and BiSrCaCuO by Weber *et al.*,[24] the signal increases dramatically when $T \lesssim T_c$. Thus, there is no a priori reason to exclude the hypothesis that these signals are due to superconductivity. However, one should notice that the magnitude of these signals are several orders of magnitude larger than

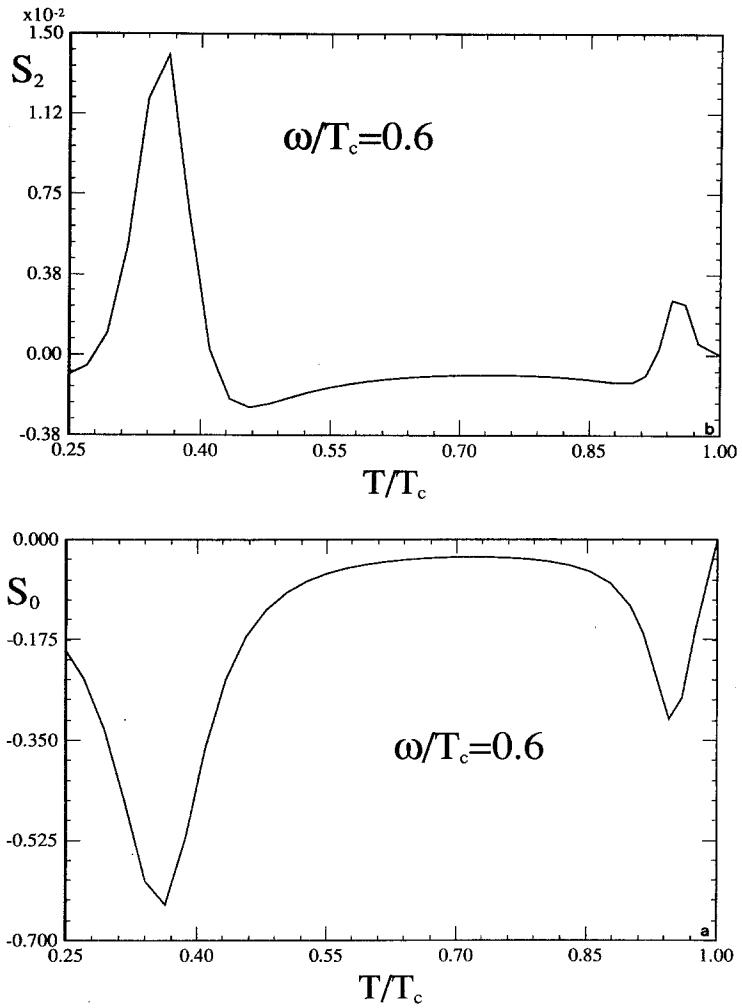


Fig. 3. The scaled Stokes parameters as functions of $t \equiv T/T_c$ at $\omega = 0.6T_c$. (a) $S_0$; (b) $S_2$; (c) $S_3$.

the theoretical values obtained here. On the other hand, no signal was reported in the experiment by Spielman *et al.*[23] Though some effects not included in the present calculation (see below) are expected to modestly increase the magnitude of the signal, the reported values are still much too large (and the operating frequencies of the experiments are much higher than the energy scale $T_c$) to be attributed to unconventional BCS superconducting states of broken 2D parity and time-reversal symmetries.

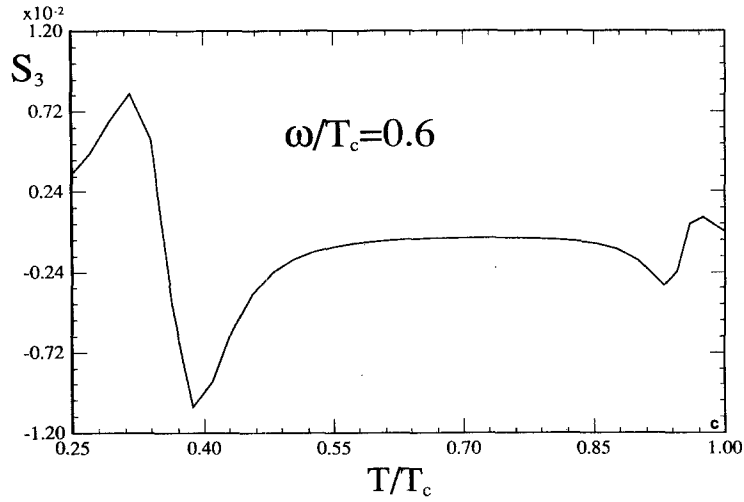


Fig. 3. Continued.

In conclusion we have investigated the possibility of observing circular dichroism and birefringence in a superconductor with the appropriate broken symmetries, and have presented a calculation for one model state, namely the ABM state. It is pointed out that the existence of the effect relies on particle–hole asymmetry, and comes from the collective response of the system. The effect is found to be very small for good type II superconductors.

Our calculations have been done for an ideal system with complete spherical symmetry. Fermi surface anisotropy will affect the position of the flapping mode resonance.[38] However, we do not expect any significant qualitative difference from this effect. Similar remarks apply to other modifications from fermi-liquid effects and weak impurity scattering. However, two possible exceptions should be noted. The amplitude of the signal near resonance is controlled by the gap nodes, thus for a cylindrical Fermi surface (as may be appropriate to the quasi-two-dimensional oxide superconductors) and for the ABM state, the magnitude of the effect (on resonance) would be significantly increased because the collective mode resonances would be much sharper. Secondly, the surface-induced distortions of the order parameter may give rise to an additional contribution to the induced current, which is difficult to estimate a priori. However, we leave the investigation of these possibilities to the future.

Recently we received a preprint by Li and Joynt[39] which also addresses the question of circular dichroism and birefringence in unconventional superconductors. Their analysis and conclusions differ significantly from ours.

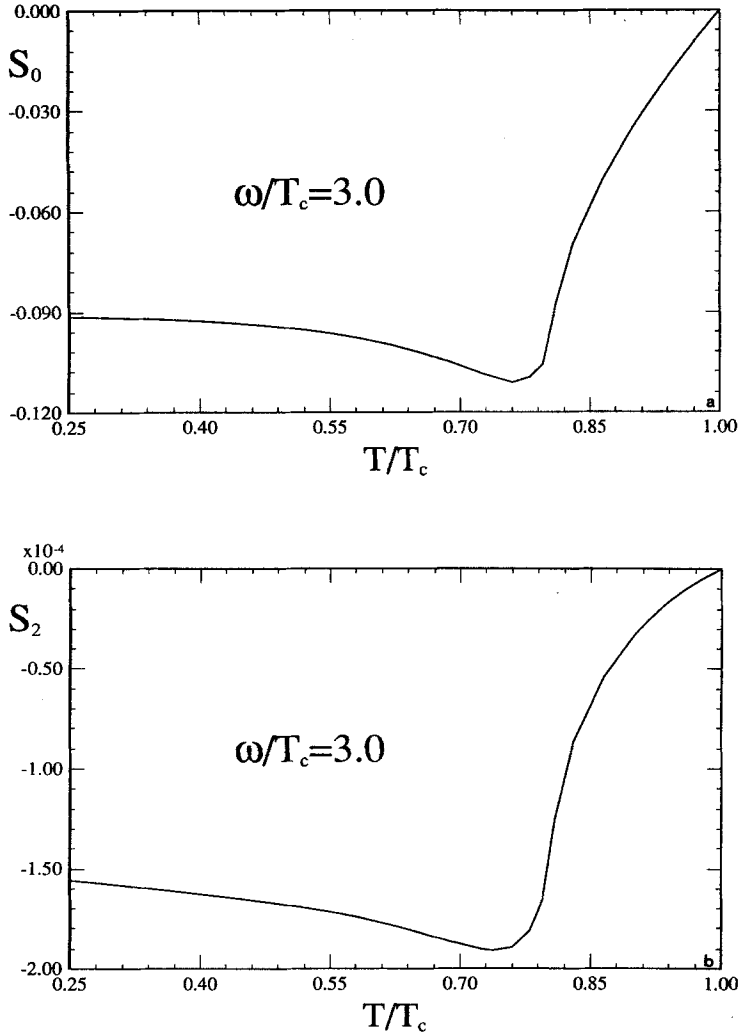


Fig. 4. The scaled Stokes parameters as functions of $t \equiv T/T_c$ at $\omega = 3T_c$. (a) $S_0$; (b) $S_2$; (c) $S_3$.

## APPENDIX I

Here we collect the formulas obtained for the solution to the linearized tansport equation, together with the definitions of the functions appearing in Eqs. (42)–(46) in Sec. 3.

The inversion of Eq. (31) yields Eq. (36) with the matrix elements of

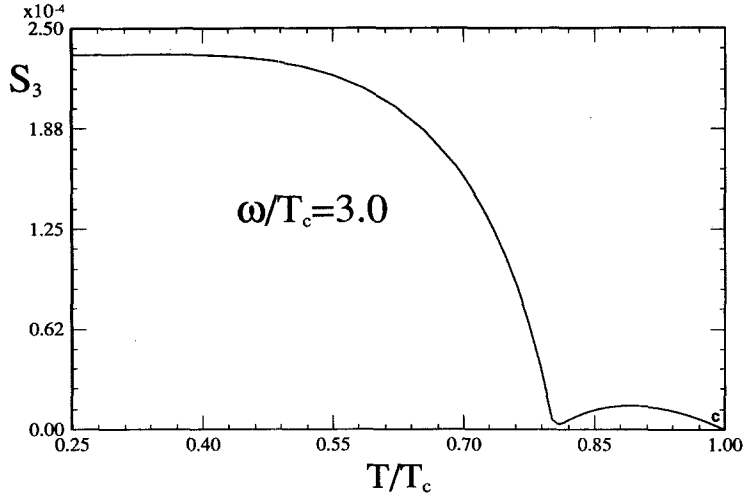


Fig. 4. Continued.

$\hat{m}(\hat{p}, \varepsilon; \mathbf{q}, \omega)$ given by

$$
\begin{aligned}
m_{11} &= -2\left(\frac{\omega}{\omega^2-\eta^2}\right)\Phi + 2\left(\frac{\eta^2}{\omega^2-\eta^2}\right)|\Delta|^2 L \\
m_{12} &= -2\left(\frac{\eta}{\omega^2-\eta^2}\right)\Phi + 2\left(\frac{\eta\omega}{\omega^2-\eta^2}\right)|\Delta|^2 L \\
m_{13} &= i\eta\Delta_I L - \left(\frac{\omega}{\omega^2-\eta^2}\right) D_\beta \Delta_R + \frac{4\eta^2|\Delta|^2}{D}\left(\frac{\omega}{\omega^2-\eta^2}\right) D_\beta \Delta_R \\
&\quad - \frac{\eta^2\omega}{D} D_\beta \Delta_R - \frac{2\varepsilon\eta^2}{D} S_\beta \Delta_R \\
m_{14} &= -\eta\Delta_R L + \left(\frac{\omega}{\omega^2-\eta^2}\right) iD_\beta \Delta_I - \frac{4\eta^2|\Delta|^2}{D}\left(\frac{\omega}{\omega^2-\eta^2}\right) iD_\beta \Delta_I \\
&\quad + \frac{\eta^2\omega}{D} iD_\beta \Delta_I + \frac{2\varepsilon\eta^2}{D} S_\beta i\Delta_I \\
m_{22} &= -2\left(\frac{\omega}{\omega^2-\eta^2}\right)\Phi + 2\left(\frac{\omega^2}{\omega^2-\eta^2}\right)|\Delta|^2 L \\
m_{23} &= i\omega\Delta_I L - \left(\frac{\eta}{\omega^2-\eta^2}\right) D_\beta \Delta_R + \frac{4\omega^2|\Delta|^2}{D}\left(\frac{\eta}{\omega^2-\eta^2}\right) D_\beta \Delta_R
\end{aligned}
\tag{75}
$$

$$-\frac{\eta\omega^2}{D} D_\beta \Delta_R - \frac{2\varepsilon\eta\omega}{D} S_\beta \Delta_R$$

$$m_{24} = \omega\Delta_R L + \left(\frac{\eta}{\omega^2-\eta^2}\right) iD_\beta\Delta_I - \frac{4\omega^2|\Delta|^2}{D}\left(\frac{\omega}{\omega^2-\eta^2}\right) iD_\beta\Delta_I$$

$$+\frac{\eta\omega^2}{D} iD_\beta\Delta_I + \frac{2\varepsilon\eta\omega}{D} S_\beta i\Delta_I$$

$$m_{33} = -\tfrac{1}{2}S_\beta - \tfrac{1}{2}(\omega^2-\eta^2-4\Delta_R^2)L$$

$$m_{34} = -2i\Delta_R\Delta_R L - \eta(\omega^2-\eta^2)\frac{\varepsilon S_\beta}{D} - \frac{\eta\omega}{2}(\omega^2-\eta^2-4|\Delta_R|^2)\frac{D_\beta}{D}$$

$$m_{44} = -\tfrac{1}{2}S_\beta - \tfrac{1}{2}(\omega^2-\eta^2-4\Delta_I^2)L$$

$$\begin{aligned} &m_{21} = m_{12} \\ &m_{31} = -m_{13}^*, \qquad m_{32} = -m_{23}^* \\ &m_{41} = -m_{14}^*, \qquad m_{42} = -m_{24}^*, \qquad m_{43} = m_{34}^* \end{aligned} \tag{76}$$

where the functions appearing in these equations are defined by

$$\begin{aligned} &\Phi(\varepsilon;\omega) = -\tfrac{1}{2}D_\alpha \\ &L(\varepsilon;\omega) = [\eta^2 S_\beta + 2\varepsilon\omega D_\beta]/D \\ &D(\varepsilon;\omega) = (4\varepsilon^2-\eta^2)(\omega^2-\eta^2) + 4\eta^2|\Delta(\hat{p})|^2 \end{aligned} \tag{77}$$

with

$$\begin{aligned} S_\alpha &= \alpha(\varepsilon+\omega/2) + \alpha(\varepsilon-\omega/2) \\ S_\beta &= \beta(\varepsilon+\omega/2) + \beta(\varepsilon-\omega/2) \\ D_\alpha &= \alpha(\varepsilon+\omega/2) - \alpha(\varepsilon-\omega/2) \\ D_\beta &= \beta(\varepsilon+\omega/2) - \beta(\varepsilon-\omega/2) \end{aligned} \tag{78}$$

Note that $S_\alpha$, $D_\beta$ ($S_\beta$, $D_\alpha$) are odd (even) functions of $\varepsilon$ and $\omega$. The particle-hole symmetric response functions appearing in Eqs. (42)–(46) are

$$\bar{\lambda}(\hat{p};\mathbf{q},\omega) = \lambda(\hat{p};\mathbf{q},\omega)/|\Delta|^2 = \int \frac{d\varepsilon}{2\pi i} L(\hat{p},\varepsilon;\mathbf{q},\omega) \tag{79}$$

and

$$\gamma(\hat{p}) = \int \frac{d\varepsilon}{4\pi i} S_\beta = \int_{-\varpi_c}^{\varpi_c} \frac{d\varepsilon}{2\pi i} \beta(\hat{p}, \varepsilon) + O\left(\frac{\omega}{\varpi}\right)^2 \tag{80}$$

which is logarithmically divergent, but can be regularized by noting that the equilibrium gap equation (22) is given by the following angular integral of $\gamma$,

$$\gamma_1 = \frac{3}{2} \int \frac{d\Omega}{4\pi} |y_+(\hat{p})|^2 \gamma(\hat{p}) = \frac{1}{V_1} \tag{81}$$

The particle–hole asymmetric functions are also logarithmically divergent and are cutoff at an energy scale $T_c \ll \varpi_c < E_f$ reflecting the origin of these terms as high-energy corrections to the low-energy transport equations. The are formally defined by the integrals

$$\mu^-(\omega) = \int_{-\varpi_c}^{\varpi_c} \frac{d\varepsilon}{2\pi i} \left(a \frac{\varepsilon}{E_f}\right) D_\beta \tag{82}$$

$$\mu^+(\omega) = \mu^- + \rho - \nu \left(1 - \frac{\omega^2}{4|\Delta|^2}\right) \tag{83}$$

$$\nu(\omega) = \int_{-\varpi_c}^{\varpi_c} \frac{d\varepsilon}{2\pi i} \left(a \frac{\varepsilon}{E_f}\right) D_\beta \left(\frac{4\omega^2|\Delta|^2}{D}\right) \tag{84}$$

$$\rho(\omega) = \int_{-\varpi_c}^{\varpi_c} \frac{d\varepsilon}{2\pi i} \left(a \frac{\varepsilon}{E_f}\right) S_\beta \left(\frac{2\varepsilon\omega^3}{D}\right) \tag{85}$$

Finally, the angular averages of these integrals that determine the response functions and dispersion relations of the collective modes are given by

$$\lambda_{mn}(q_z, \omega) = \frac{3}{2} \int \frac{d\Omega}{4\pi} |y_m(\hat{p})|^2 p_z^n \Delta(T)^2 \bar{\lambda}(\hat{p}) \tag{86}$$

$$\gamma_m(\omega) = \frac{3}{2} \int \frac{d\Omega}{4\pi} |y_m(\hat{p})|^2 \gamma(\hat{p}) \tag{87}$$

Note that although the integrals $\gamma_m$ are logarithmically divergent, they enter the equations of motion for the order parameter only in linear combinations that are convergent, or that can be regularized by the equilibrium gap equation (cf. Eq. (49)).

## APPENDIX II

In this appendix we record some of the technical details used to evaluate the integrals given in Appendix I. We handle the temperature dependence

of the various integrands by transforming to Matsubara frequencies via

$$\frac{1}{2\varepsilon}\tanh\left(\frac{\varepsilon}{2T}\right)=T\sum_{\varepsilon_n}\frac{1}{\varepsilon_n^2+\varepsilon^2} \tag{88}$$

where $\varepsilon_n=(2n+1)\pi T$. For example, the first term in Eq. (49) for the normal-flapping mode frequencies can be transformed to

$$\gamma_0-\gamma_1=3\left\langle\int_{-\infty}^{\infty}d\xi\ T\sum_{\varepsilon_n}\left(\frac{1}{\varepsilon_n^2+\xi^2+|\Delta(\hat{p})|^2}-\frac{1}{\varepsilon_n^2+\xi^2}\right)(|y_0(\hat{p})|^2-|y_+(\hat{p})|^2)\right\rangle \tag{89}$$

where the angle brackets denote an angular average. Note that we have regularized the integral by subtracting off a term which would give zero after angular integration. The $\xi$-integration can now be performed, leaving a rapidly convergent Matsubara sum and angular integration which can be done numerically.

After we expand to leading order in $(q_z v_f/\omega)^2$, all of the particle–hole symmetric functions can be expressed in terms of integrals of the form

$$F_n=\left\langle\int_{-\infty}^{\infty}\frac{d\varepsilon}{2\pi i}\frac{\beta(\varepsilon)}{4\varepsilon^2-\omega^2}p_z^n\right\rangle \tag{90}$$

Using Eq. (88) we can rewrite this integral as

$$F_n=\left\langle\int d\xi\ 2T\sum_{\varepsilon_n}\frac{1}{4\xi^2+4|\Delta(\hat{p})|^2-\omega^2}\frac{1}{\xi^2+\varepsilon_n^2+|\Delta(\hat{p})|^2}p_z^n\right\rangle \tag{91}$$

One needs to pay careful attention to the zeros of the denominator in Eq. (91) by interpreting $\omega\to\omega+i\delta$ with $\delta\to 0$. The $\xi$-integral must be performed separately for the two cases, $\omega^2\gtrless 4|\Delta(\hat{p})|^2$. A straightforward calculation yields

$$F_n=\left\langle\left\{2\pi T\sum_{\varepsilon_n}\frac{1}{\varepsilon_n^2+\omega^2/4}\left[\frac{\Theta(4|\Delta(\hat{p})^2|-\omega^2)}{\sqrt{(4|\Delta(\hat{p})^2|-\omega^2)}}+i\frac{\Theta(\omega^2-4|\Delta(\hat{p})^2)|}{\sqrt{(\omega^2-4|\Delta(\hat{p})^2)|}}\right]\right.\right.$$
$$\left.\left.-\pi T\sum_{\varepsilon_n}\frac{1}{\sqrt{\varepsilon_n^2+|\Delta(\hat{p})|^2}}\frac{1}{\varepsilon_n^2+\omega^2/4}\right\}p_z^n\right\rangle \tag{92}$$

The angular integration is twice the integral carried out over the half sphere, $p_z>0$, since the ABM gap function is given by $|\Delta(\hat{p})|^2=\Delta(T)^2(1-p_z^2)$. The square-root singularities, which occur for $\omega<2\Delta(T)$, are handled by a

change of variables; $\hat{p}_z = z_0 - t^2$ and $\hat{p}_z = z_0 + t^2$, respectively, with $z_0 = \sqrt{1-(\omega/2\Delta(T))^2}$. The resulting angular integrals are

$$F_n = \frac{1}{\Delta(T)}\left\{\frac{2\pi}{\omega}\tanh\left(\frac{\omega}{4T}\right)\left(\int_0^{\sqrt{z_0}} dt\,\frac{2(z_0-t^2)^n}{\sqrt{2z_0-t^2}} + i\int_0^{\sqrt{1-z_0}} dt\,\frac{2(z_0+t^2)^n}{\sqrt{2z_0+t^2}}\right)\right.$$
$$\left. - \int_0^1 dt\left(2\pi T\sum_{\varepsilon_n}\frac{1}{\varepsilon_n^2+\omega^2/4}\,\frac{t^n}{\sqrt{a_n^2-t^2}}\right)\right\} \qquad \text{if } \omega < 2\Delta(T) \tag{93}$$

or

$$F_n = \frac{1}{\Delta(T)}\left\{\frac{2\pi}{\omega}\tanh\left(\frac{\omega}{4T}\right)\left(+i\int_0^1 dt\,\frac{t^n}{\sqrt{z_1^2+t^2}}\right)\right.$$
$$\left. - \int_0^1 dt\left(2\pi T\sum_{\varepsilon_n}\frac{1}{\varepsilon_n^2+\omega^2/4}\,\frac{t^n}{\sqrt{a_n^2-t^2}}\right)\right\} \qquad \text{if } \omega > 2\Delta(T) \tag{94}$$

where

$$z_1 = \sqrt{\left(\frac{\omega}{2\Delta(T)}\right)^2 - 1} \qquad \text{and} \qquad a_n = \sqrt{1+\frac{\varepsilon_n^2}{\Delta(T)^2}}.$$

Thus, $F_n$ is reduced to a rapidly convergent sum and simple integral, which can be evaluated easily on a computer. The particle–hole asymmetric terms can be integrated by parts and expressed in terms of the integrals $F_n$ and angular integrals of $\gamma_{\hat{p}}$.

## ACKNOWLEDGMENT

This research is supported by the Science and Technology Center for Superconductivity through NSF grant number DMR 88-09854. We also thank the Aspen Center for Physics, where the final version of the manuscript was prepared.

## REFERENCES

1. J. Bardeen, L. N. Cooper, and R. Schrieffer, *Phys. Rev.* **108**, 1175 (1957).
2. P. W. Anderson, *Basic Notions of Condensed Matter* (Benjamin Cummings, Menlo Park, 1984).
3. L. P. Gorkov, *Sov. Sci. Rev.* **A9**, 1 (1987).
4. D. Rainer, *Phys. Scr.* **T23**, 106 (1988).
5. M. Sigrist and K. Ueda, *Rev. Mod. Phys.* **63**, 239 (1991).
6. J. Annett, *Adv. Phys.* **39**, 83 (1990).
7. A. J. Leggett, *Rev. Mod. Phys.* **47**, 331 (1975).
8. L. P. Gorkov, *JETP Lett.* **40**, 1155 (1984).

9. C. H. Choi and P. Muzikar, *Phys. Rev.* **B37**, 5947 (1988).
10. P. Hirschfeld, *Phys. Rev.* **B37**, 9331 (1988).
11. B. Arfi, H. Bahlouli, and C. J. Pethick, *Phys. Rev.* **B39**, 8959 (1989).
12. R. Joynt, *Sup. Sci. Tech.* **1**, 210 (1988).
13. D. Hess, T. Tokuyasu, and J. A. Sauls, *J. Phys. Cond. Matt.* **1**, 8135 (1989).
14. K. Machida and M. Ozaki, *J. Phys. Soc. Jpn.* **58**, 2244 (1989).
15. E. Blount, C. Varma, and G. Appeli, *Phys. Rev. Lett.* **64**, 3074 (1990).
16. C. H. Choi and P. Muzikar, *Phys. Rev.* **B39**, 9664 (1989).
17. T. Tokuyasu, D. Hess, and J. A. Sauls, *Phys. Rev.* **B41**, 8891 (1990).
18. V. Kalmeyer and R. B. Laughlin, *Phys. Rev. Lett.* **59**, 2095 (1987).
19. B. I. Halperin, J. March-Russell, and F. Wilczek, *Phys. Rev.* **B40**, 8726 (1989).
20. X. G. Wen and A. Zee, *Phys. Rev. Lett.* **62**, 2873 (1988).
21. K. B. Lyons, J. Kwo, J. F. Dillon Jr., G. P. Espinosa, M. McGlashan-Powell, A. P. Ramirez, and L. F. Schneemeyer, *Phys. Rev. Lett.* **64**, 2949 (1990).
22. K. B. Lyons, J. F. Dillon Jr., E. S. Hellman, E. H. Hartford, and M. McGlashan-Powell, *Phys. Rev.* **B43**, 11408 (1991).
23. S. Spielman, K. Fesler, C. B. Eom, T. H. Geballe, M. M. Fejer, and A. Kapitulnik, *Phys. Rev. Lett* **65**, 123 (1990).
24. H. J. Weber, D. Weitbrecht, D. Brach, A. L. Shelankov, H. Keiter, W. Weber, Th. Wolf, J. Geerk, G. Linker, G. Roth, P. C. Splittgerber-Hünnekes, and G. Güntherodt, *Sol. State Comm.* **76**, 511 (1990).
25. P. W. Anderson and P. Morel, *Phys. Rev.* **123**, 1911 (1961).
26. R. McKenzie and J. A. Sauls, *Helium Three* (Elsevier, Amsterdam, 1991), p. 255.
27. W. P. Halperin and E. Varoquauz, *Helium Three* (Elsevier, Amsterdam, 1991), p. 353.
28. J. W. Serene, *Quantum Fluids and Solids* (American Institute of Physics, New York, 1983), p. 305.
29. R. S. Fishman and J. A. Sauls, *Phys. Rev.* **31**, 251 (1985).
30. G. Eilenberger, *Z. Phys.* **214**, 195 (1968).
31. G. M. Eliashberg, *Sov. Phys.–JETP* **34**, 668 (1972).
32. A. I. Larkin and Yu. N. Ovchinnikov, *Sov. Phys.–JETP* **28**, 1200 (1969).
33. J. W. Serene and D. Rainer, *Phys. Rep.* **101**, 221 (1983).
34. P. Wölfle, *Prog. in Low Temperature Physics VIIA* (North-Holland, Amsterdam, 1983).
35. P. Wölfle, *Physica* **90B**, 96 (1977).
36. P. J. Hirschfeld, P. Wölfle, D. Einzel, J. Sauls, and W. Puttika, *Phys. Rev.* **B40**, 6695 (1989).
37. P. Wölfle and V. E. Koch, *J. Low. Temp. Phys.* **30**, 61 (1978).
38. H. Monien, K. Scharnberg, L. Tewordt, and N. Schopohl, *J. Low. Temp. Phys.* **65**, 13 (1986).
39. Q. P. Li and R. Joynt, *Phys. Rev.* **B44**, 4720 (1991).